CARBON FOAMS AS CATALYST SUPPORTS FOR PHENOL PHOTODEGRADATION

LF. Velasco[b], B. Tsyntarski[a], B. Petrova[a], T. Budinova[a], N. Petrov[a], JB. Parra[b], CO. Ania[b*]

[a] Institute of Organic Chemistry, Bulgarian Academy of Sciences, Acad. G. Bonchev Str. Bl. 9, 1113 Sofia, Bulgaria

[b] Instituto Nacional del Carbón (INCAR), CSIC, Oviedo 33080, Spain

[*]Corresponding author E-mail: conchi@incar.csic.es (CO Ania)

Tel.: +34 985118846; Fax: +34 985297662

Abstract

In this work we have synthesized a carbon foam prepared using coal tar pitch as precursor, and investigated its utilization as catalyst support for the immobilization of titanium oxide. The performance of the carbon foam/titania catalyst was investigated towards the photodegradation of phenol from aqueous solution, and the results compared to those of pure titania and supported on an activated carbon. Despite the relatively low surface area of the carbon foam, the supported photocatalyst displays an efficient photodegradation of phenol after 4 hours of UV irradiation, similar to that attained using a high surface activated carbon as support. At short reaction times, the photodegradation efficiency is higher in the activated carbon composite. In contrast, both catalysts perform very similar under long irradiation times, pointing out to a kinetic limitation for phenol degradation on the carbon foam supported catalyst. Although the nature the degradation intermediates is the same in all the studied catalysts, their concentrations differ significantly. When titania is supported on the carbon foam large amounts of catechol are detected in solution after UV irradiation, which indicates a better degradation efficiency. Moreover, phenol photodegradation rate over both carbon/titania catalysts outperformed that attained in non-supported titania.

Keywords

carbon foam, photocatalysis, titania, phenol

1. INTRODUCTION

One of the most important challenges for science is to develop efficient methods to control environmental pollution, particularly to remove hazardous organic compounds from water resources. Heterogeneous photocatalysis has proven to be a promising method for the degradation of these compounds, being titania (TiO_2) the most commonly used photocatalyst,

because it is non-toxic, photo-stable, cheap and very efficient under ultraviolet light irradiation (its band gap energy of 3.2 eV requires photoexcitation in the near-UV spectrum region) [1]. The reaction mechanisms and the electron/hole generation processes involved in photocatalytic reactions using titania have been widely studied and can be found in a number of reviews [2,3].

However TiO_2 powders present some drawbacks as the powders are not easy to precipitate and recover from water, preventing their regeneration and reuse. Therefore, during the past few decades, many efforts have been devoted to develop strategies oriented to the large-scale implementation of this technology for water treatment, especially with regards to effective methods to separate the nanosized photocatalyst from water streams. Several engineering solutions are currently being investigated, from incorporating titania on the reactor walls and the use of slurry reactors coupled to post-reaction separation processes, to immobilization techniques on different supports [4-8].

In this regard, the use of carbon-TiO_2 catalysts has currently attracted much attention for the photocatalytic degradation of toxic pollutants. Mixtures of different forms of porous carbons (among them activated carbons, carbon nanotubes, activated carbon fibers and nanofibers) and TiO_2 have been widely studied [9-13]. The photoactivity of carbon-titania composites -provided by TiO_2 particles- is strongly dependent on the features of the carbon material. For instance, the high porosity of the carbon support provides an effective adsorption of the pollutants on the catalyst surface, and therefore it might accelerate the process of their decomposition through the transfer of the adsorbed molecules to the surface of the photoactive titania. On the other hand, the hydrophobic/hydrophilic nature of the support may also control the stability of the catalyst and interactions between the titania and the carbon support. Indeed, the immobilization of the photoactive titanium oxide on carbon materials has been reported to show a synergistic effect for the photodegradation of organic pollutants [14-16]. Additionally, other authors have reported that the presence of activated carbons actually changes the TiO_2 catalytic behavior beyond this synergistic effect on the degradation kinetics [17, 18]. On the other hand, high surface catalysts may also be advantageous since the basic photocatalytic effects are most likely to occur at the catalyst-water interface (or nearby) [18], and thus the immobilization of TiO_2 on a porous substrate would yield a higher activity photocatalyst.

The aim of this work was to investigate the application of carbon foams obtained from coal tar pitch as a support for the immobilization of TiO_2 for the photodegradation of phenol in aqueous solutions. The choice of carbon foams as support is made upon their structural characteristics; they can be synthesized as rigid materials with a moderate surface area comprised of an interconnected network. As probe molecule we have selected phenol, one of the most refractarious aromatic compounds frequently found in wastewater. The efficiency of the carbon-titania catalyst in the photo-assisted degradation of phenol in aqueous solutions was discussed in terms of the chemical and textural properties of the carbon supports.

2. EXPERIMENTAL

2.1 MATERIALS SYNTHESIS

The carbon foam was synthesized using coal tar pitch as precursor, which was first submitted to a chemical modification in concentrated H_2SO_4 at 120ºC until solidification. This modification of the precursor composition causes an increase in the viscosity and softening point of the coal tar pitch, which allows the foaming process to be conducted at atmospheric pressure. The obtained solid product was heated at atmospheric pressure up to 600 ºC in a covered silica crucible under nitrogen atmosphere (heating rate 10 ºC min^{-1}), yielding a rigid vitreous carbon foam. The obtained foam was further submitted to steam activation at 800 ºC for 1 h for promoting the development of a more open porous structure. The sample after activation is denoted as CF. Additionally, a commercial activated carbon AC (physical activation of bituminous coal) was also used for comparison purposes (particle size 0.212-0.710 mm). This carbon is characterized by a low oxygen content (ca. 2.1 wt.%) and a basic nature (point of zero charge of 8.9 pH units).
The titania-carbon catalysts were prepared by infiltration of a suspension in ethanol of commercial titanium oxide (P25 Degussa) on the carbon material (weight ratio carbon: titania 90:10) in a rotary evaporator under vacuum for 2 hour. After the rotation, the solvent (ethanol) was evaporated out. The samples were labeled as XTi, being X the reference to the carbon support: AC for the commercial activated carbon and CF for the carbon foam. Bare TiO_2 was also used as a standard for comparison purposes. Before usage, all the samples were washed in distilled water at 60 ºC, dried at 110 ºC overnight and kept in a desiccator.

2.2 CHARACTERIZATION

Nanotexture of both the carbon support and the titania/carbon composites was characterized by N_2 (ASAP 2010, Micromeritics) adsorption isotherms at -196 ºC. Before the experiments, the samples were outgassed under vacuum (ca. 10^{-3} torr) at 120 °C overnight. The isotherms were used to calculate the specific surface area, S_{BET}, and pore volumes using the t-plot method using a carbon-coated Sooty-silica as reference material [19]. The as-received carbon and the carbon/titania composites were further characterized by thermogravimetric analysis using a Setaram Labsys thermal analyzer. The instrument settings were as follows: heating rate 15 ºC min^{-1} and a N_2 atmosphere with 50 mL min^{-1} flow rate.
The morphology of the composites was characterized using a Ziess DSM 942 scanning electron microscope. The carbon particles were dispersed on a graphite adhesive tab placed on an aluminum stub. The images were generated in the backscattered electron signal mode, which yielded better quality pictures.

2.3 ADSORPTION AND PHOTODEGRADATION OF PHENOL

Phenol photodegradation experiments under UV irradiation were followed by means of kinetics studies from batch experiments at room temperature. Photocatalytic reaction conditions were previously optimized concerning the initial phenol concentration, catalyst loading, and time of irradiation. Briefly, about 1 g L^{-1} of catalyst was placed in a photoreactor of 400 mL capacity, containing an aqueous solution of phenol (distilled non buffered water) of initial concentration 100 mg L^{-1} (solution pH ca. 6 units). The UV irradiation source was provided by a high pressure mercury lamp (125 W), vertically suspended in a cylindrical, double-walled quartz jacket cooled by flowing water, immersed in the solution. The water cell was used to control the temperature during the experiments, preventing any overheating of the suspension due to the irradiation. The suspensions were stirred (500 rpm) during the UV irradiation and small aliquots of the solution (~1 mL) were taken out at fixed time intervals and analyzed by reverse-phase HPLC (Spherisorb C18, 125 mm x 4 mm), using methanol-water mixtures as mobile phase, and a photodiode array detector. The samples were previously filtered using regenerated cellulose filter having mean pore size of 0.45 μm.

Dark adsorption (in the absence of UV irradiation) was also carried out under the same experimental conditions than UV irradiation, in order to counterbalance the fraction of photodecomposed phenol from that adsorbed on the pores of the carbon/titania catalysts.

3. RESULTS AND DISCUSSION

CHARACTERIZATION OF THE CATALYST SUPPORTS

The performance of carbon foams as catalyst support for phenol photodegradation was evaluated and discussed in terms of their textural and chemical features. For this purpose, supported catalysts with a carbon:titania (weight ratio 90:10) were prepared by immobilization of commercial titanium oxide (P25 Degussa) as detailed in the experimental section. The ratio support:titania was chosen based on preliminary optimization studies concerning the activity of various catalysts with carbon loading (not published results). The carbon-based catalysts along with fresh titanium oxide (P25) were characterized by means of gas adsorption (Table 1).

The morphology of the catalysts was also investigated by SEM (Figure 1). The wall structure of the carbon foam obtained after the pyrolysis of modified coal tar pitch is characterized by a reticular vitreous structure, indicative of a closed cell structure. These reticulated characteristics have also been observed in foams prepared by pyrolysis of polymers, and pitches of coal extracts [20]. Such close-cell foams typically show a smooth surface with a low porosity at a nanometric scale. In agreement with this, the textural analysis revealed a poorly developed porosity (surface area 26 m^2 g^{-1}).

After steam activation, a slight opening of the carbon matrix occurred and CF sample displayed a porous open structure of interconnected pores with a moderate surface area (ca. 375 $m^2 g^{-1}$) and a micro/mesoporous structure. This sample was then selected for incorporating the photoactive catalyst. Additionally, the SEM micrographs of the composites (Figure 1) show that titanium oxide is well dispersed over the carbon support, with particles of a few tens of nm in size comparable to those of the (non-supported) photocatalyst.

The immobilization of titania on the carbon foam partially blocked the initial porosity of the support (ca., 50 % decrease in surface area and pore volumes), although the sample still displays a somewhat porous character (Table 1). A deeper insight into the porous features of the catalyst reveals that the modification affected mostly the microporosity, determined by N_2 adsorption data, indicating that titania is incorporated in the inner micropores of the carbon support during the impregnation, rather than remaining on the outer surface. In contrast, when titania is immobilized on a high surface area and microporous activated carbon support, the porous features of the composite are not substantially reduced. Similar observations have been reported in the literature [9, 10, 15, 17] about the immobilization of titanium oxide on porous carbon substrates.

Since the immobilization is based on a physical interaction/adsorption (no chemical bonding is expected), it is important to control any leaching out the photoactive particles during the photodegradation experiments from solution (which indeed was not observed). In this regard, weak interactions (like charge transfer) seem to be occurring between the carbon support and titania; this was confirmed by determined pH_{PZC} of the carbon supports after the immobilization of titania. Their initial basic nature (pH_{PZC} varies between 9-10 units in the non-doped carbon supports) was slightly modified after the incorporation of titania (pH_{PZC} 6.8 and 7.3 units for ACTi and CFTi, respectively).

PHENOL PHOTODEGRADATION

It has to be considered that for a porous catalyst, the removal efficiency encompass both adsorption and degradation; so the performance under UV irradiation should also be compared to that in dark conditions (absence of UV irradiation). For this reason, phenol removal efficiency on the studied catalysts was evaluated by kinetic measurements under both dark and UV irradiation conditions (Figure 2).

Upon adsorption in dark conditions on the carbon supports and the carbon/titania composites, the expected concentration decline curves due to retention of phenol molecules on the materials' surface were obtained. Analysis of the species in solution confirmed that no phenol degradation occurs under dark conditions, regardless the catalyst used. In the case of pure titania, the amount of phenol adsorbed was very low (removal efficiency below 3 %), which is in good agreement with its non-porous nature (Table 1).

In contrast, phenol removal efficiency at dark conditions on both carbon:titania composites cannot be disregarded, as it reached almost 70 % after 6 hours for ACTi, as opposed to 28 % in the case of CFTi sample. This evidence is consistent with the porous features of both catalysts: the higher surface area and pore volume of sample ACTi results in a much higher adsorption capacity of the aromatic compound. However, the rate of adsorption under dark conditions appeared to be faster in the carbon foam composite -compared to ACTi catalyst- despite the poor porous development of CFTi. In fact, 80% of phenol adsorption in sample CFTi takes place within the first 30 min of contact with the solution, as opposed to ACTi (ca. 30 %). This suggests that most of the surface area in the CFTi (and thus the adsorption sites) is readily accessible to the phenol molecules and that external diffusion is favoured when the carbon foam is used as support.

Analysis of the porous features of the carbon/titania catalysts after phenol exposure under dark conditions (Table 1) reveals that a significant fraction of the porosity of these materials still remains unoccupied after phenol loading (ca. less than 25 % is occupied). Even though it seems that both catalysts have reached their maximal phenol adsorption capacity in the experimental conditions carried out (based on the shape of the kinetic curves shown in Figure 2), most of the pore volume of the catalysts remains unblocked.

The thermal analysis of the preadsorbed catalysts at dark conditions confirmed the presence of phenol inside the porous matrix in both cases (Figure 3), with an overall mass loss of 4 and 1 wt.% for ACTi and CFTi, respectively. Besides the desorption peak corresponding to the evolution of moisture (centered at 100 ºC), the profiles show only one peak -centred at about 300ºC- corresponding to desorption of phenol retained in the catalysts. Similar DTG profiles have been obtained for the preadsorption of phenol at dark conditions on the carbon supports themselves (not shown), indicating that the incorporation of the titania on the carbon support does not substantially change the phenol adsorption sites present on the porous carbon matrix.

On the other hand, when UV irradiation is applied, phenol removal efficiency is significantly improved in all the catalysts. While the rate of phenol photodegradation on P25 follows an almost linear trend, the supported catalysts exhibit faster and higher removal efficiencies (Figure 2). This tendency was more remarkable in the early stages of the process, although the final overall yield after 6 hours of irradiation was rather high in all the cases (i.e., 75 % for P25 after 6 hours of irradiation, vs over 95 % for both carbon supported photocatalysts). Thus, it appears that the immobilization of TiO_2 on the porous carbon support enhances the photoactivity of titania particles. What is more significant is that - although some differences are observed at short times - phenol degradation efficiency in both carbon:titania photocatalysts is similar after 3 hours of UV irradiation.

The enhancement in phenol removal upon irradiation can be regarded as a sequential two-steps process: a rapid concentration of phenol on the surface of the support- due to the preferential

adsorption on the solid phase- followed by a spontaneous transfer of adsorbed phenol molecules from the support to titania surface, where it is decomposed as a consequence of the UV irradiation. This enhanced photoactivity as a result of the combination of the adsorption on a carbon support and the photoactivity of titanium oxide has been described in the literature, when using activated carbons as additive to titania in the photodegradation of organic pollutants [14, 17, 21, 22].

It should not be forgotten that for the porous catalysts, a fraction of the degradation compounds (even phenol itself) might be retained (adsorbed) inside the pores, as opposed to the case of TiO_2, where all degradation intermediates are necessarily detected in the solution. For this reason, we have analyzed the likely textural changes occurred in the catalysts after the adsorption and the photodegradation process (dark and UV series in Table 1). Gas adsorption data revealed that the high phenol removal efficiencies detected after UV irradiation were not accompanied by a pore plugging effect. Although the amount of removed phenol in the photodegradation experiments increased up to 95-99 % (from 66 and 28 % under dark conditions), the decrease in the porosity of the catalysts is very similar in both experiments (photodegradation and dark adsorption). This suggests that phenol is not relocated inside the porous network of the photocatalysts; it appears to be either fully mineralized or decomposed as small size intermediates that are not so readily retained in the pores of the carbon support.

The DTG profiles (Figure 3) of the composites after phenol photodegradation also confirm this observation. The small mass loss values obtained in the catalysts (i.e., 1.9 and 1 wt.% for ACTi and CFTi, respectively) indicate that small amounts of gases evolve from the catalysts after phenol photodegradation (even lower than those at dark conditions). Neither phenol itself nor the aromatic intermediates created during the photodegradation were detected on the catalysts surface.

Analysis of the solution composition during irradiation of the catalysts allowed the extent of phenol degradation to be determined. When P25 is irradiated along with the decrease in phenol concentration in solution, rising amounts of p-benzoquinone (BZ), hydroquinone (HQ) and catechol (CAT) were detected (Figure 4). The occurrence of these intermediates for phenol photodegradation using Degussa P25 is in good agreement with reported works in the literature [23]. Although all of them are detected at very low concentrations (below 0.5 mmol L^{-1}), BZ and HQ are the dominant intermediates, particularly at the earlier stages of the reaction. Both compounds showed a concentration peak between 1-2 hours, whereas upon longer irradiation times their concentration decreased slightly, suggesting that they are also decomposed. In contrast, increasing concentrations of CAT are detected along the whole irradiation time, although at concentrations below 10 micromol L^{-1}. Since P25 is a non-porous material, degradation intermediates remain in the solution where they should be necessarily detected. On the other hand, we cannot discard the presence of the formation of smaller degradation

intermediates (such as short alkyl chain organic acids), that are not detected by reverse-phase HPLC in a standard C18 column, which was the analytical technique used to identify, separate and quantify the intermediates.

The nature of the degradation intermediates detected when the carbon supported photocatalysts are irradiated did not changed, although they were obtained in different proportions (Figure 4).

Increasing amounts of HQ, BZ and CAT were detected after UV irradiation of ACTi and CFTi, similarly to non-supported titania. With the exception of CAT, these intermediates are detected at lower concentrations than those in P25, thus confirming that supporting titanium oxide on porous carbon materials enhance the overall phenol photodegradation efficiency.

What is more interestingly inferred from this study is that, based on the identification and quantification of the intermediate products detected in the aqueous solution (Figure 4), the carbon supports appear to modify the phenol photodegradation pathway. For instance, BZ and HY being the predominant intermediates for P25 are now only detected during the first hour of irradiation of ACTi and CFTi, and at about 10 times lower concentration -whereas in the case of P25 their concentration remained somewhat constant up to 3 hours and then started to fall at a slow rate. The third intermediate product detected during the irradiation of P25 -traces of CAT- was now found to be predominant in both carbon catalysts, with concentrations about 8 times higher during almost the whole time of irradiation. Comparing the two composites investigated, the carbon foam gives rise to a higher amount of intermediates during the degradation, which concentration dependence with time follows the sequence: CAT>> HY>>BZ. This effect is particularly more remarkable in the case of CAT and could be due to a faster release of the generated intermediates in the solution, as a consequence of the less developed porous network of this support. However, the concentration of intermediates detected in solution was also higher in ACTi sample -compared to P25- which possess a higher porosity where a priori intermediates could be retained (adsorbed). Moreover, the amount of organic compounds remaining in the solution after 6 hours of irradiation of CFTi is almost negligible (Table 2), and comparable to that of the activated carbon composite with a higher surface area.

These results provide an interesting viewpoint on the photocatalytic degradation of phenol, indicating that the degradation reaction would mainly occur in the interface carbon/titania/solution. Thus the eventual beneficial effect of a highly porous supported catalyst does not seem to rule this system. On the contrary, accessible porosity for preventing mass transfer limitations of the pollutants from the bulk solution are required.

On the other hand, conversion of phenol to CAT has been reported to be more advantageous for the complete mineralization of phenol than conversion to BZ or HY [24, 25], because catechol is decomposed to oxalic acid, and then to CO_2 and water, whereas the pathways of mineralization of BQ and HQ proceeds through the formation of a large number of intermediates (mainly non-aromatic acids such as maleic, malonic, oxalic and formic acid). Based on the higher amounts of

CAT detected when using the carbon supported photocatalysts -and particularly in CFTi sample- are irradiated, it might be anticipated that the degradation of phenol is more efficient on the carbon foam based photocatalyst -although short alkyl chain organic acids have not been quantified and will be further studied in ongoing works.

These results confirm that supporting titanium oxide on porous carbon materials does not only enhance the overall phenol degradation efficiency (so-called synergistic effect), but also modifies the degradation pathway of this aromatic compound. Evidences, reporting that an activated carbon support may induce different interactions between titania and phenol molecules, had been reported in the literature [12].

On the other hand, the synergetic effect of carbon supports has been mostly correlated to the porosity of the support [14, 15, 22]. Our results show that high porous features on the supported catalysts are not decisive. In fact, high phenol photodegradation efficiency can be obtained using a low surface area carbon foam as support for the dispersion on titania nanoparticles. Even if the adsorption capacity of the carbon support towards of the target pollutant under dark conditions is low (i.e. 275 vs 668 micromol/mg for CFTi and ACTi, respectively), high photodegradation efficiencies are achieved. So this parameter would seem to be more related to the amount of titania incorporated in the photocatalyst.

4. CONCLUSIONS

Carbon foams with a moderate porous development are excellent supports for the immobilization of titania, since the obtained catalysts present an enhanced photoactivity towards phenol degradation. Despite its moderate porous features, the performance of the carbon foam supported catalyst is comparable to that of a catalyst supported on a commercial activated carbon with higher porosity.

Identification of the degradation intermediates released in the solution demonstrated that besides supporting titanium oxide on porous carbon materials does not only enhance the overall phenol degradation efficiency via increasing the removal rate. The presence of the carbon support also brings about a modification in the degradation route of this compound, compared to the photodegradation activity of titania. Moreover, higher amounts of catechol are detected in the solution when titania is supported on the carbon foam, suggesting a more efficient phenol degradation on this catalyst. This points out that the degradation would mainly occur in the interface carbon/titania/solution; consequently, high surface area supports are not necessary, but an accessible pore structure that avoids mass transfer limitations or kinetic diffusion restrictions for the accessibility of the pollutants from the bulk solution to the interface support/titania.

ACKNOWLEDGMENTS

This work was supported by the Spanish MICINN (CTM2008-01956). LFV thanks CSIC for a predoctoral fellowship. The authors acknowledge the support of Bulgarian MEYS -contracts MU01-149-.

REFERENCES

[1] H. Choi, E. Stathatos, D. Dionysiou, Sol-gel preparation of mesoporous photocatalytic TiO_2 films and TiO_2/Al_2O_3 composite membranes for environmental applications. Appl. Catal. B 63 (2006) 60-67.

[2] D.F. Ollis, H. Al-Ekabi (Eds.), Photocatalytic Purification and Treatment of Water and Air, Elsevier, Amsterdam, 1993.

[3] E. Pelizzetti, N. Serpone (Eds.), Photocatalysis: Fundamental and Applications, Wiley, New York, 1989.

[4] M. Mohseni, Gas phase trichloroethylene (TCE) photooxidation and byproduct formation: photolysis vs. titania/silica based photocatalysis, Chemosphere, 59, (2005) 335-342.

[5] A. Fernández, G. Lassaletta, V.M. Jiménez, A. Justo, A.R. Gonzàlez-Elipe, J.M. Herrmann, H. Tahiri, Y. Ait-Ichou, Preparation and characterization of TiO_2 photocatalysts supported on various rigid supports (glass, quartz and stainless steel). Comparative studies of photocatalytic activity in water purification, Appl Catal B: Environ. 7 (1995) 49-63.

[6] L. Erdeia, N. Arecrachakula, S. Vigneswaran, A combined photocatalytic slurry reactor-immersed membrane module system for advanced wastewater treatment, Sep. Purif. Technol. 62 (2008), 382-388.

[7] F. Sunada, A. Heller, Effects of water, salt water, and silicone overcoating of the TiO_2 photocatalyst on the rates and products of photocatalytic oxidation of liquid 3-octanol and 3-octanone, Environ Sci Technol. 32 (1998) 282–286.

[8] N. Takeda, N. Iwata, T. Torimoto, H. Yoneyama, Influence of carbon blacks of carbon black as an adsorbent used in photocatalyst films on photodegradation behaviors of propyzamide, J Catal 177 (1998) 240-246.

[9] B. Tryba, A.W. Morwski, M. Inagaki, Application of TiO_2-mounted activated carbon to the removal of phenol from water, Appl. Catal. B 41 (2003) 427-433.

[10] B. Tryba, Photocatalytic Activity of TiO_2 by Carbon and Iron Modifications, Int. J. Photoenergy 721824 (2008) 1-15.

[11] C.G. Silva, W. Wang, J.L. Faria, Photocatalytic and photochemical degradation of mono-, di- and tri-azo dyes in aqueous solution under UV irradiation, J. Photochem. Photobiol. A: Chem. 181 (2006) 314-324.

[12] J. Araña, J. M. Doña-Rodríguez, E. Tello Rendón, C. Garriga i Cabo, O. González-Díaz, J. A. Herrera-Melián, J. Pérez-Peña, G. Colón, J. A. Navío, TiO_2 activation by using activated carbon as a support: Part II. Photoreactivity and FTIR study, Applied Catalysis B: Environmental, 44 (2003) 153-160.

[13] N. Keller, G. Rebmann, E Barraud, O.Zahraa, V. Keller, Macroscopic carbon nanofibers for use as photocatalyst support, Catalysis Today 101 (2005) 323-329.

[14] J. Matos, J. Laine, J.-M. Herrmann, D. Uzcategui, J.L. Brito, Influence of activated carbon upon titania on aqueous photocatalytic consecutive runs of phenol photodegradation, Applied Catalysis B: Environmental, 70 (2007) 461-469.

[15] J. Matos, J. Laine, J.M. Herrmann, Synergy effect in the photocatalytic degradation of phenol on a suspended mixture of titania and activated carbon, Appl. Catal. B 18 (1998) 281-291.

[16] X. Zhang X, M. Zhou, L. Lei, TiO_2 photocatalyst deposition by MOCVD on activated carbon, Carbon 44 (2006) 325-333.

[17] L.F. Velasco, J.B. Parra, C.O. Ania, Role of activated carbon features on the photocatalytic degradation of phenol. Appl. Surf. Sci. 2010 (in press)

[18] J. Cunningham, G. Al-Sayyed, S. Srijaranai In: G.R. Helz, R.G. Zepp and D.G. Crosby, Editors, Aquatic and Surface Photochemistry, Lewis, Boca Raton, FL (1994), pp. 317–348.

[19] P.J.M. Carrott, R.A Roberts, K.S.W. Sing, Standard Adsorption Data for Non-Porous Carbons, Carbon, 25 (1987) 769-770.

[20] C. Chen, E.B. Kennel, A.H. Stiller, P.G. Stansberry, J.W. Zondlo, Carbon foam derived from various precursors. Carbon 44 (2006) 1535-1543.

[21] S.X. Liu, X.Y. Chen, X. Chen, A TiO2/AC composite photocatalyst with high activity and easy separation prepared by a hydrothermal method, J. Haz. Mat. 143 (2007) 257-263.

[22] T. Cordero, J.M. Chovelon, C. Duchamp, C. Ferronato, J. Matos, Surface nano-aggregation and photocatalytic activity of TiO2 on H-type activated carbons, Appl. Catal. B: Environ. 73 (2007) 227-235.

[23] E.B. Azevedo, A.R. Torres, F.R. Aquino Neto, M. Dezotti, TiO2-Photocatalyzed degradation of phenol in saline media in an annular reactor: hydrodynamics, lumped kinetics, intermediates, and acute toxicity. Braz. J. Chem. Eng.26 (2009) 75-87.

[24] A. Santos, P. Yustos, A. Quintanilla, F. Garcia-Ochoa, Kinetic model of wet oxidation of phenol at basic pH using a copper catalyst, Chem. Eng. Sci., 60 (2005) 4866-4878.

[25] A. Santos, P. Yustos, A. Quintanilla, S. Rodríguez and F. Garcia-Ochoa, Route of the catalytic oxidation of phenol in aqueous phase, Appl. Catal. B: Environ. 39 (2002) 97-113.

Figure 1. A) Image of the carbon foam synthesized from coal tar pitch at atmospheric pressure and SEM micrographs of the materials used as catalysts and supports: B) sample P25; C) sample CF; D) sample CFTi; E) sample AC; F) sample ACTi.

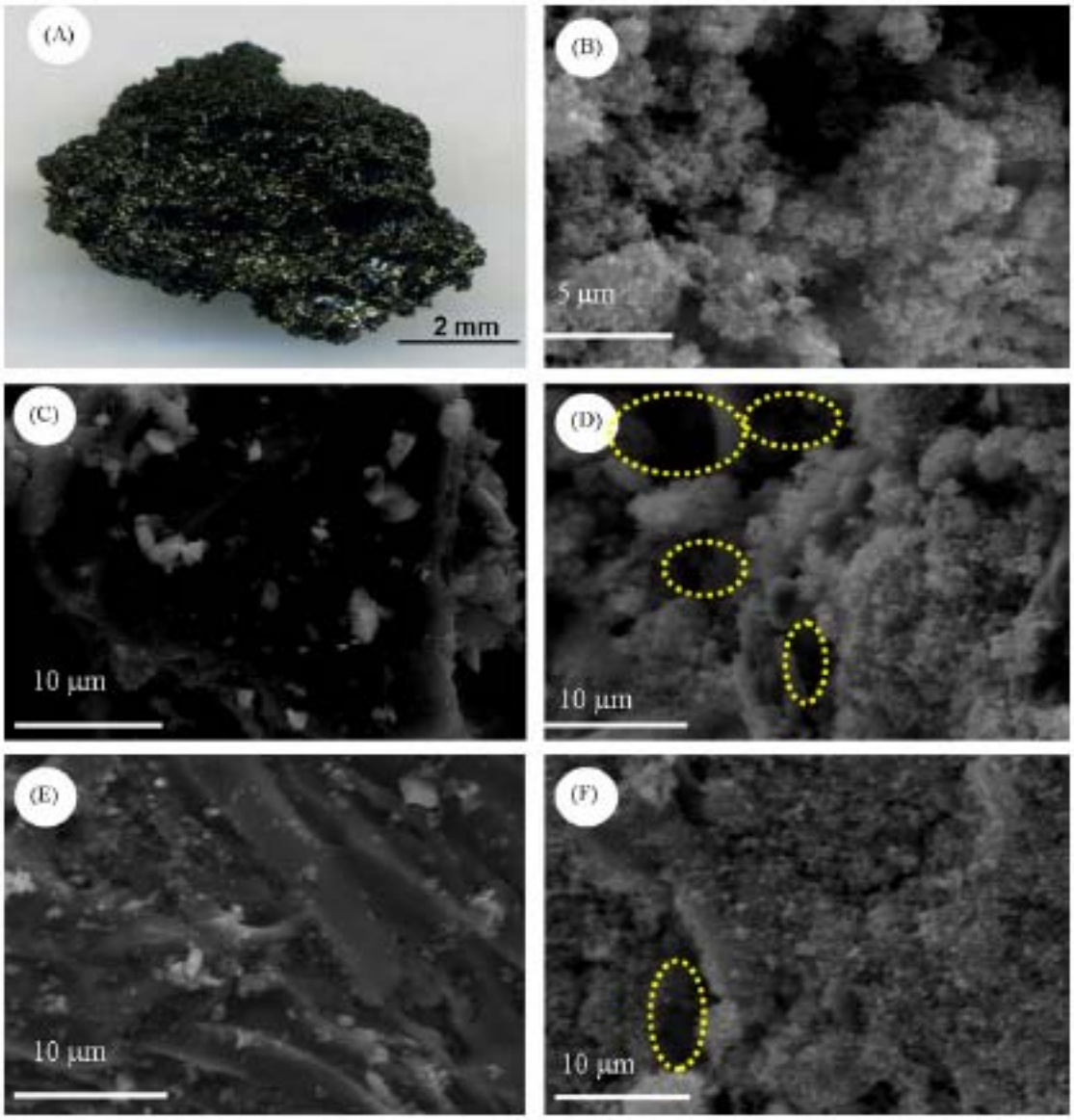

Figure 2. Phenol concentration decay curves on the investigated photocatalysts after dark adsorption and UV irradiation.

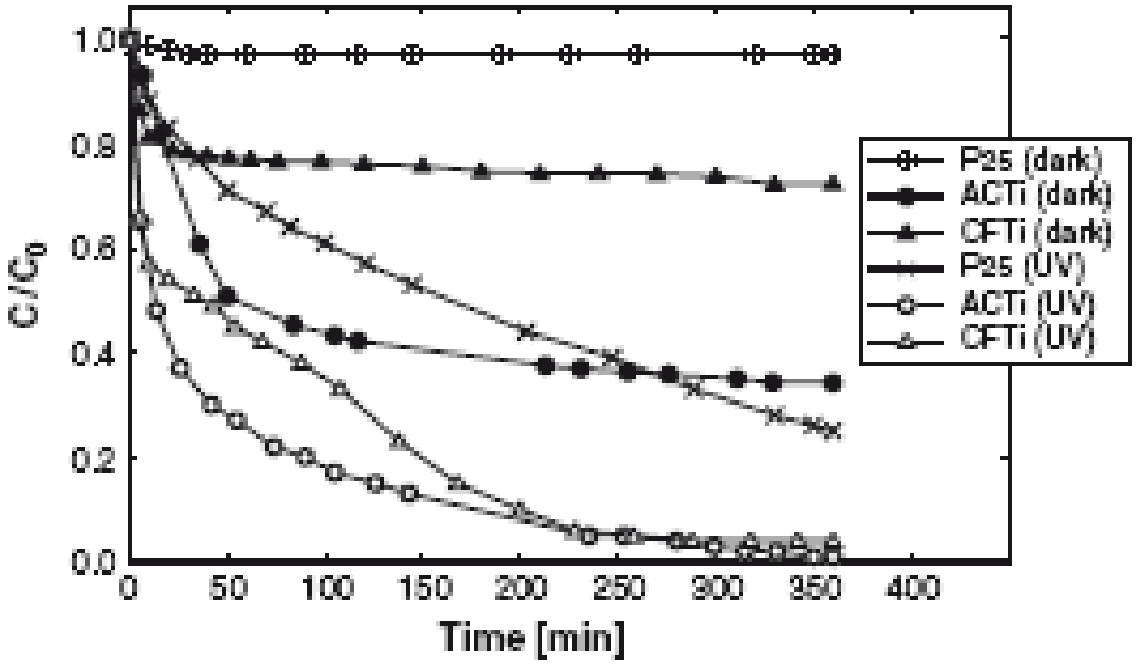

Figure 3. DTG profiles of the studied carbon:titania catalysts after phenol removal under dark conditions and UV irradiation.

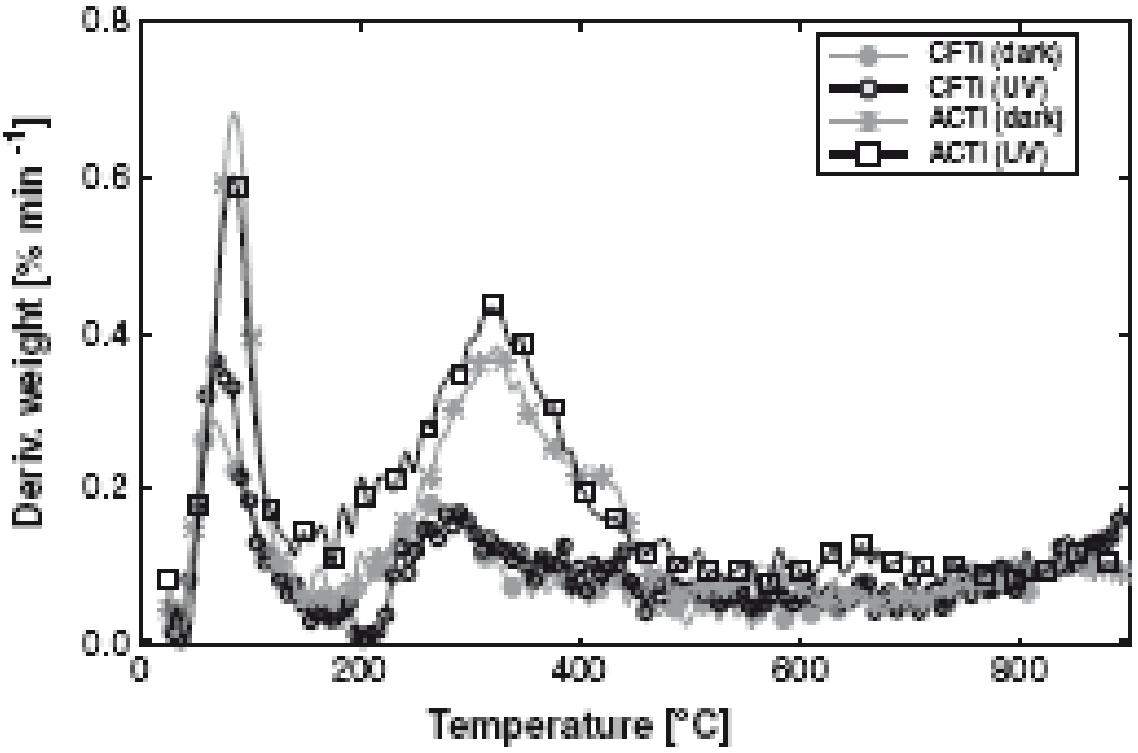

Figure 4. Evolution of the concentration of phenol degradation intermediates (BZ, HY and CAT) upon UV irradiation of the different investigated photocatalysts.

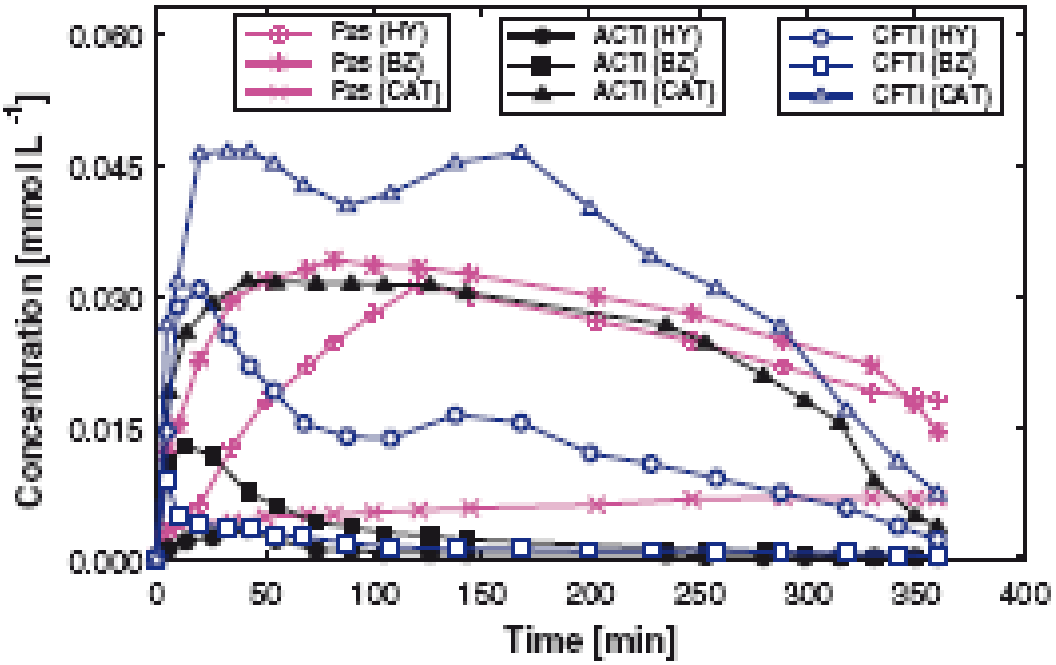

Table 1
Textural parameters obtained from N_2 adsorption isotherms at −196 °C of the as-received catalysts, and after phenol removal under dark conditions (dark series) and UV irradiation (UV series).

	S_{BET} [$m^2\ g^{-1}$]	V_{TOTAL}[a] [$cm^3\ g^{-1}$]	$V_{MICROPORES}$[b] [$cm^3\ g^{-1}$]	$V_{MESOPORES}$[b] [$cm^3\ g^{-1}$]
P25	53	0.118	–	–
CFTi	165	0.109	0.074	0.019
ACTi	924	0.497	0.458	0.054
CFTi (dark)	146	0.096	0.069	0.016
ACTi (dark)	760	0.400	0.330	0.043
CFTi (UV)	103	0.068	0.049	0.012
ACTi (UV)	780	0.400	0.339	0.039

[a] Evaluated at relative pressures of 0.99.
[b] Evaluated by t-plot method.

Table 2
Apparent first-order rate constants (k_{app}), half reaction time ($t_{1/2}$), initial reaction rate (r_0) and correlation coefficient (R^2) obtained from fitting experimental data to the Langmuir–Hinshelwood model.

	$k_{app} \times 10^2$ [min^{-1}]	$t_{1/2}$ [min]	$r_0 \times 10^3$ [min^{-1}]	R^2 [min^{-1}]	Remarks	Reference
P25 (UV)	3.5	197	3.8	0.992	Solution: 100 ppm phenol	
ACTi (UV)	10.6	65	10.9	0.982	UV lamp: 125 W	This work
CFTi (UV)	9.3	74	10.0	0.972	Carbon:titania ratio 9:1 Catalyst 1 $g L^{-1}$	
P25	5.6	–	–	–	Solution: 100 ppm phenol	
TiO_2–AC_M	13.9	–	–	–	UV lamp: 125 W	[14,15]
TiO_2–AC_{PC}	4.6	–	–	–	Carbon:titania ratio 1:5 Catalyst 3 $g L^{-1}$	
Bare-TiO_2	3.1	–	–	–	Solution: 100 ppm phenol	
23-AC–TiO_2	2.5	–	–	–	UV lamp: 4 × 15 W Carbon:titania ratio 23:77 Catalyst 2 $g L^{-1}$	[12,24]
P25	1.7	–	–	–	Solution: 100 ppm phenol	
TiO_2–CA	7.7	–	–	–	UV lamp: 20 W	[25]
TiO_2–sol–gel	1.5	–	–	–	Carbon:titania ratio 1:2 Catalyst 1.5 $g L^{-1}$	

Table 3
Quantification of phenol degradation intermediates [$\mu mol L^{-1}$] remaining in the solution after 6 h of reaction under dark conditions (dark series) and UV irradiation (UV series). Phenol initial concentration was 1000 $\mu mol L^{-1}$ for all the samples.

	Total [$\mu mol L^{-1}$]	Phenol [$\mu mol L^{-1}$]	HY [$\mu mol L^{-1}$]	BZ [$\mu mol L^{-1}$]	CAT [$\mu mol L^{-1}$]
P25 (dark)	970	970	n.d.	n.d.	n.d.
P25 (UV)	294	253	18	16	7
CFTi (dark)	723	723	n.d.	n.d.	n.d.
ACTi (dark)	340	340	n.d.	n.d.	n.d.
CFTi (UV)	46	36	2	0.3	8
ACTi (UV)	18	11	0	4	4